Silica-based UV-fibers for DUV applications: current status

K.-F. Klein[1,5], C.P. Gonschior[1,5], D. Beer[1], H.-S. Eckhardt[2], M. Belz,[3]
J. Shannon[4], V.Khalilov[4], M.Klein[5], C.Jakob[5]
[1] Technische Hochschule Mittelhessen - University of Applied Sciences,
W.-Leuschner-Str. 13, 61169 Friedberg, Germany
email: Karl-Friedrich.Klein@iem.thm.de
[2] tec5 AG, 61440 Oberursel, Germany
[3] World Precision Instruments Deutschland GmbH, 61169 Friedberg, Germany
[4] Polymicro Technologies, Sub. of Molex, Inc., Phoenix, AZ 85023, US
[5] TransMIT GmbH, Center of fiber-optics and industrial laser applications,
Saarstr. 23, 61169 Friedberg, Germany

ABSTRACT

The current status of UV-damage in several different UV fibers due to defects in their synthetic high-OH silica core and cladding will be described. Further, steps to improve UV resistance and adequate measurement techniques based on a deuterium lamp setup are included. For the first time, the main parameters and their influences on UV induced losses are discussed in detail with an emphasis towards future standardization purposes.
Applications based on two new UV light sources, a laser driven xenon plasma broad band source and a high pulse-power 355 nm Nd:YAG laser, are introduced. UV photo-darkening and -bleaching in UV fibers caused by this extremely powerful light source is demonstrated. Finally, first results on transmission of UV light in optical fibers at cryogenic temperatures are shown.

Keywords: step-index fibers, multimode fibers, UV-fibers, low solarization deuterium lamp, broadband light-source, 355 nm laser, UV-applications, fiber-optic delivery system, cryogenic temperatures, standardization.

1. INTRODUCTION

Multimode fibers with an undoped silica core and a fluorine-doped silica cladding are commonly used for the transmission of UV-light from a multitude of different UV-light sources. However, over the last decades, only broadband continuous-wave (cw) deuterium-lamps have been used to quantify UV-induced transmission losses and quality improvements in optical fibers with core diameters ranging from 200 µm to 600 µm (or even larger) [1-7]. In parallel, the improving performance of fiber optic spectrometers, dipping probes, gas and liquid flow cells for fluid injection analysis and HPLC absorbance detection have been studied [8-19].

Although the measurement-techniques to quantify UV induced transmission damage were continuously developed and improved, only little activities in respect to standardization of methods determining such UV-damages of silica-based fibers were reported. Therefore, the current status of UV-fibers and the related measurement techniques including the main critical parameters will be shown in the following. Finally, two new applications currently under studies will be introduced.

2. DEFECTS IN UV-FIBERS WITH UNDOPED SILICA CORE

Defects in silica [1-4,20-24] can be generated by ionizing radiation, such as Gamma-rays, X-rays or DUV-light. Spectral UV-induced losses generated by deuterium-lamps and excimer-lasers have been investigated for the last two decades. Based on these studies in the UV-region, only some optically active defects were found in undoped synthetic silica, as seen in Table 1. Especially E'-centers (≡Si$^{\bullet}$: silicon with one unpaired electron) with an absorption band at 214 nm and Non-Bridging-Oxygen-Hole centers NBOHC (≡Si-OH°) at 260 nm are well known in high-OH silica (see table 1).

Micro-structured and Specialty Optical Fibres II, edited by Kyriacos Kalli,
Jiri Kanka, Alexis Mendez, Proc. of SPIE Vol. 8775, 87750B · © 2013 SPIE
CCC code: 0277-786X/13/$18 · doi: 10.1117/12.2020993

In addition, Oxygen-Deficient-Centers (ODCs) around 250 nm are observed in low-OH silica. An overview about UV-defects is given in [20-24,25-27].

The synthetic fused silica used as core material in common step index UV fibers is an extremely pure material. However, several intrinsic and impurity defects are present in varying concentrations. These defects differ between low and high OH fibers [2,5,21,26]; in Table 1, an overview about defects in high OH fibers is given. In addition, certain defects in the silica structure can be caused by ionizing irradiation (Table 2 for high OH fibers). The concentration of each defect is dependent on several factors, including preform contaminants, preform manufacturing technique and fiber draw process

Table 1: Overview about defects in high OH fibers

Defect Description	**Chemical Structure**	**Comment**
-OH in Silica structure	≡ Si - OH HO - Si ≡	Stable configuration
Strained Silica bond	≡ Si – O - Si ≡	Weakened regular bonds
Chlorine impurity	Cl - Cl	Absorption band at 320nm
HCl impurity	H - Cl	Absorption band near 165nm
SiH impurities	Si – H	Precursor

Table 2: Radiation induced defects in high OH fibers

Defect Description	**Chemical Structure**	**Comment**
E' center	≡ $Si^{\bullet}$	Absorption band at 214nm
Non Bridging Oxygen Hole Center (NBOHC)	≡ Si - O°	Absorption bands at 260nm and 620nm
Silicon without unpaired electron	≡ Si^{+}	Absorption band at 163nm

3. MANUFACTURING OF UV-FIBERS AND PROPERTIES IN UV REGION

UV fibers for applications below 250 nm commonly used are step-index fibers with an undoped synthetic silica core surrounded by a fluorine-doped silica cladding. These fibers are manufactured in several steps. A rod of high-OH synthetic silica is produced by flame-hydrolysis [7] using silicon tetrachloride in an oxygen-hydrogen burner. With Plasma Outside deposition (POD) this UV preform is cladded with silica having a fluorine content of approx. 3%; to obtain a Cladding-Core-Ratio, CCR, typically in the order of 1.1 or smaller [7]. Such performs with diameters > 15 mm are drawn into fibers, with core diameters between 50 to 1000 µm. To improve UV optical performance, additional preform and fiber treatments can be carried out.

In 1993, standard UV fibers (type: FVP [6]; 1st generation) drawn from standard UV preforms [7] had a very low basic attenuation, with values of < 1.0 dB/m at 200 nm. However, these fibers were darkened below 230 nm during UV irradiation with deuterium lamps; the UV induced losses at 214 nm of 1 m long fibers were between 10 to 40 dB, depending on different manufacturing and testing parameters. Over several design generations, the UV damage at 214 nm wavelength of high-OH fibers has been reduced significantly (table 3).

Table 3: History of different high-OH fibers with reduction of UV-induced losses at 214 nm

Generation	Fiber/ preform type	UV-induced loss at 214 nm in 2 m long fibers	Comments
1	FVP [6]/Standard [7]	20 … 40 dB	Start
2	UVI	< 1 dB	Hydrogen loading of fibers; lowest solarization temporarily out gassing leads to FVP fiber
3	UVM [6]/ SBU [7]	< 6.5 dB	Preform modifications
4	FDP [6]	< 1.0 dB for 200 … 600 µm core	Preform and fiber modifications

4. CHARACTERISATION OF MEASUREMENT SETUP FOR UV-DAMAGE TESTS

4.1 Overview about influencing parameters and test procedure

In Fig.2, a typical setup for testing the UV damage of fibers during UV irradiation with deuterium lamp is shown; this setup was used during R&D to confirm the performance improvements and for quality control. All spectral measurements were performed using a standard deuterium (D_2) lamp DO660/05J from Heraeus Noblelight [28] as a broadband light source and an optimized imaging system (LS). The distal end of the fiber under test (FuT) was coupled into a fiber-optic spectrometer (FOS) USB4000 from Ocean Optics [29] with an UV-enhanced grating for deep-UV used as detector system (DS). This entire system for measuring the spectral UV-induced losses at room temperature is described in detail elsewhere [4,30,31].

To enable measurements below 195 nm caused by oxygen absorption, the entire optical setup was placed in a gas-tight box and purged with nitrogen gas, allowing reliable measurements down to 170 nm. The position of the shutter (Sh) was controlled by software via electrical TTL output of a computer. Two cases were distinguished. The photo-darkening of the FuT with D_2 lamp was measured with an open shutter. During recovery phase after UV damage, the deuterium irradiation was blocked to avoid additional damage. Only during measurements, the shutter was shortly opened for 2 … 5 s, only; within this small interval in comparison to the long period of darkness, the UV damage is negligible [4,30,31].

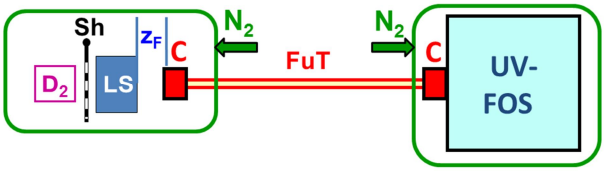

Fig. 2: Measurement setup for damaging the UV-fibers, with the following components: D2: deuterium lamp; LS: lens system; C. SMA-connector; FuT: fiber under test; UV-FOS: fiber-optic spectrometer with deep UV detection; z_F: axial distance between lens system and fiber front face; N_2: nitrogen purge, if needed.

Spectra from 185 up to 500 nm will be measured. The FOS signal FOSS(λ,t) is proportional to the spectral power densities, at a given wavelength. However, the transfer factor from input power or density to photo current or charge is strongly wavelength dependent. The spectral and temporal UV-induced losses (unit: dB) can be determined as follows:

$$L(\lambda,t) = 10 * \log (FOSS(\lambda,t=0) / FOSS(\lambda,t)) \quad (1).$$

Either, the spectral losses L (λ) at given times t_i or the temporal losses L (t) at given wavelengths λ_i are shown in the diagrams.

Although the setup appears to be simple, several parameters have to be controlled. The temporal and spectral damage of UV fibers are depending on the following parameters: deuterium lamp systems, spectral distribution with and without nitrogen purge, coupling position of the fiber, fiber lengths and temperature. In addition to permanent losses, recovering or transient defects are measurable, too. This is very important information for a variety of applications, where fiber optics are used in duty cycles. Then the transient losses have to be determined and documented, too.
Further, the measurement error for UV-induced losses was estimated to be < 0.3 dB, independent of fiber type and length. Finally, it must be considered that the dynamic range of the system is wavelength-dependent and in the order of approx. 25 dB for wavelengths > 200 nm. However, with lower wavelengths and reduced photosensitivity of the array, the dynamic range is decreasing. Especially, below 200 nm stray light causes a systematic measurement error.

Because there is no optical absorption band in high OH silica at 330 nm, this wavelength is used to compensate drift of the D_2 lamp, especially for long test runs.

4.2 Different D_2 lamps

To maximize deep UV light coupling, a light source system consisting of a D_2 lamp (DO660/05J produced by Heraeus Noblelight [28]) and a lens-based imaging system was designed for these experiments. It proved to be very efficient in generation of UV defects in high OH UV fibers below 300 nm. In Fig. 3, the main absorption band at 214 nm is dominant with a maximum of about 5 dB after 4 h of irradiation, using our standard FuT, FDP, with 5 m length.
For comparison, a commercially available broadband deuterium-halogen fiber optic light source (L10290, Hamamatsu [32]) was evaluated. The FOS signals in the inset of Fig. 3 indicate that the spectral power of the commercial light source was significantly lower for wavelengths < 210 nm. As a consequence, the 214 nm UV-induced loss is lower, too.

In addition to the spectral curves, the temporal behavior of selected wavelengths (e.g. 214, 229, 245, 254 and 265 nm) gives additional details about maximum loss or saturation. In Fig. 4, the saturation level at 214 nm is reached after approx. 2 hours with the in-house setup, whereas the 214 nm loss measured with the commercial broadband light source did not saturate in this time frame. The loss and the gradient are smaller by at least a factor of three.
For control purposes to see power fluctuations, the reference signal at 330 nm showed that the stability of the D_2 lamp with less than 0.15 dB is adequate; on first view, these fluctuations are wavelength independent.

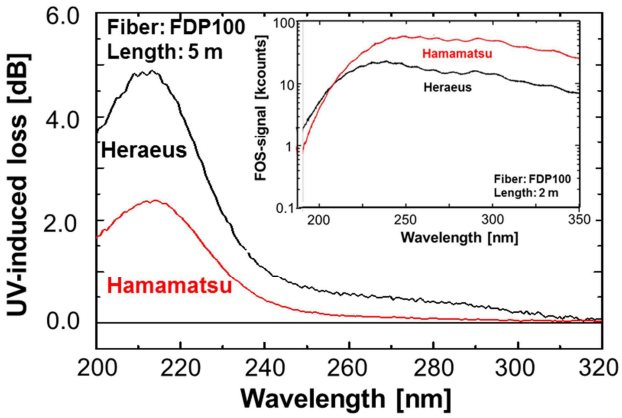

Fig. 3: Spectral UV-damage after 4 h UV irradiation, using the different deuterium lamps; in the inlet: Comparison of two deuterium-lamps with different spectral output powers using a 100 µm core fiber and a fiber-optic spectrometer

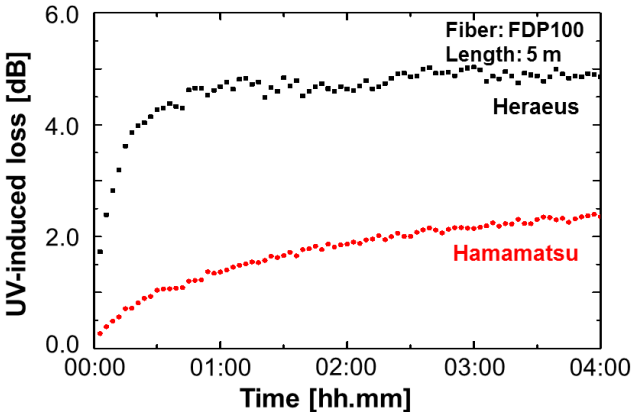

Fig. 4: Temporal UV-damage at 214 nm wavelength of the same 100 µm core fiber, using the different deuterium lamps in Fig. 2

4.3 Different power levels due to plasma current and nitrogen purge

The spectral power can be easily changed with two variations. The lamp current with recommended value of 300 mA can be varied between 270 to 350 mA, increasing the spectral power proportional to the increase of lamp current. In the deep UV below 195 nm, the power will be increased by nitrogen omitting absorption of oxygen.

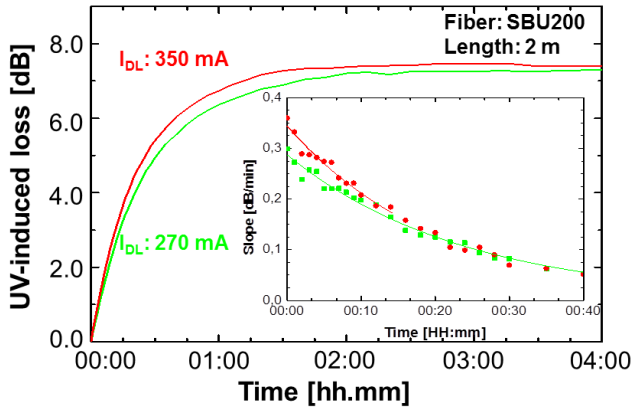

Fig. 5: Temporal UV-damage at 214 nm wavelength of 2 m long SBU-fiber with 200 µm core, using different electrical current (270 & 350 mA) for the same deuterium lamp; in the inset, the slope of both curves is shown

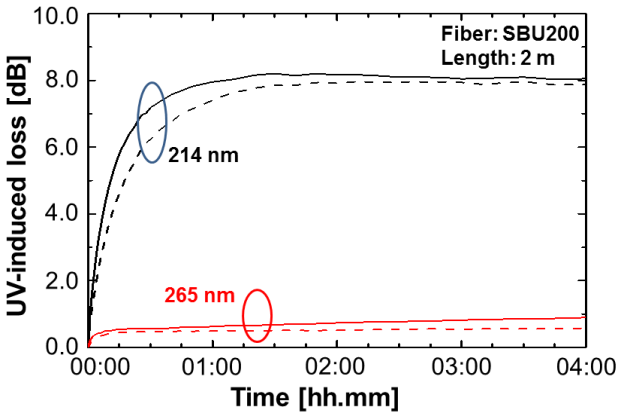

Fig. 6: Temporal UV-damage at 214 and 265 nm wavelength of2 m long SBU-fiber with 200 µm core fiber without (dashed) and with N2-purging (solid line), using 270 mA electrical current for the deuterium lamp

The influences are shown in Fig. 5 and 6, using a 2 m long SBU-fiber (3rd generation) with 200 µm core. In both cases, the final 214 nm values after 4 h UV irradiation are only slightly higher: less than 0.3 dB at approx. 8 dB. However, the starting slope at t = 0h is significantly higher: as shown in the inlet in Fig. 5, this slope will increase proportional to the current: 0.28 dB/min vs. 0.35 dB/min. In Fig. 6, the 214 nm slope increases by a factor of 2, if oxygen absorption below 195 nm is suppressed. While the 214 nm values are saturated within 4 h, the 265 nm absorption is still increasing with approx. 0.07 dB/h.

4.4 Different axial position of fiber front face

In the wavelength range of interest, spectral aberrations of the lens system have to be taken into account. This means that the focal point is decreasing with increasing refractive indices of the lenses due to decreasing wavelength. The entire spectrum is changing if the fiber input is moved in axial direction, as shown with a 600 µm fiber (Fig. 7) and 100 µm fiber (Fig. 8). Using a test system with bandpass filter and UV enhanced silicon detector, described in [2,4], the distance was adjusted for maximum power at 214 nm wavelength. Increasing the distance ($z_F > 0$), the maximum above 225 nm increases significantly Decreasing the distance, the overall signal decreases at wavelength above 225, but increased slightly at wavelength below 214nm. It is obvious, that the input angle given by the lens-system and the far field angle at the output are wavelength-dependent; for the optimized wavelength (here: 214 nm at $z_F = 0$), these angles are equal to the acceptance angle or numerical aperture at this wavelength.

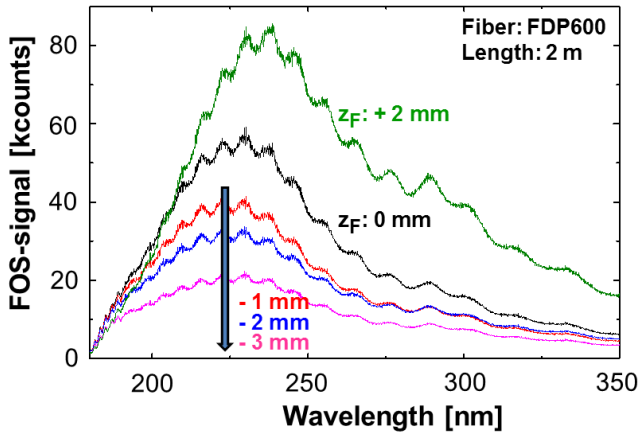

Fig. 7: *Measured spectral output power of 2 m long FDP-fiber with 600 µm core for different axial positions (z_F= 0 mm: optimized for 214 nm); the spectral coupling efficiency is determined; however, the numerical aperture at fiber input and output is wavelength-dependent; the integration time and the FOS-signal were taken in account for z_F = 2 mm*

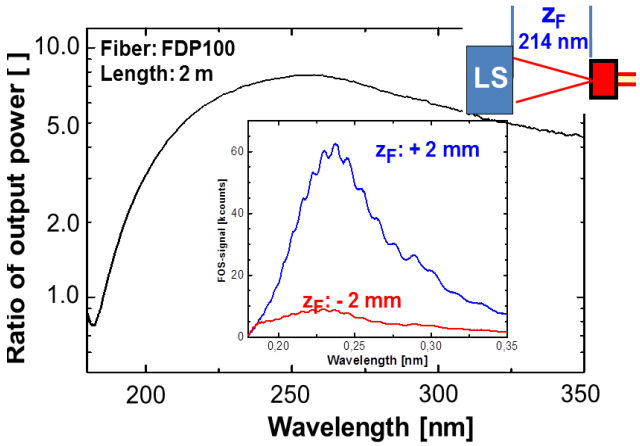

Fig. 8: *Ratio between the spectral output powers of 2 m long FDP-fiber with 100 µm core for two different axial positions (see inset); the axial position z_F= 0 mm is optimized for 214 nm; the inset show the measured output spectrum for the two extreme position different z_F= - 2 mm (optimized for < 200 nm) and = + 2 mm (optimized for > 230 nm)*

The influence of UV damage at 214 nm is shown in Fig. 9, based on signal changes in Fig. 8. As expected, the slope at the beginning is significantly different for different axial positions z_F: 0.19 dB/min (+2 mm), 0.29 dB/min (0 mm) and 0.61 dB/min (- 2mm). Interestingly, the fiber reacts with a dampened to overshoot response respectively, similar to traditional control system response, indicating two competing effects. The maximum values are different; with smaller distances, the overshoot is increasing from not existing up to 0.55 dB, absolutely, or 30%, relatively. However, the values after 4 h UV-irradiation are nearly the same with differences less than 0.1 dB, well within the estimated measurement error of 0.3 dB.

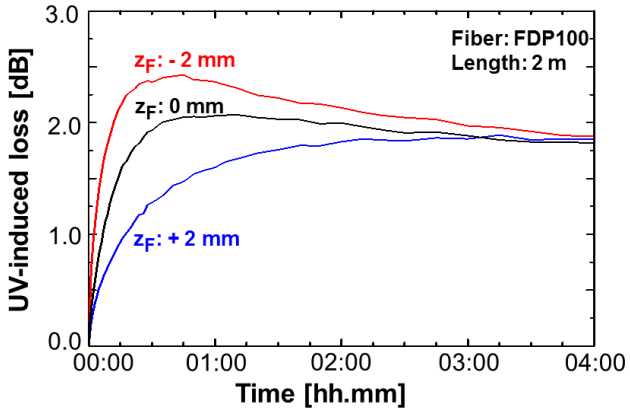

Fig. 9: Comparison of temporal UV-damage at 214 nm wavelength of 2 m long FDP-fiber with 100 µm core, for different axial position z_F (z_F= 0 mm: maximum coupling efficiency at 214 nm)

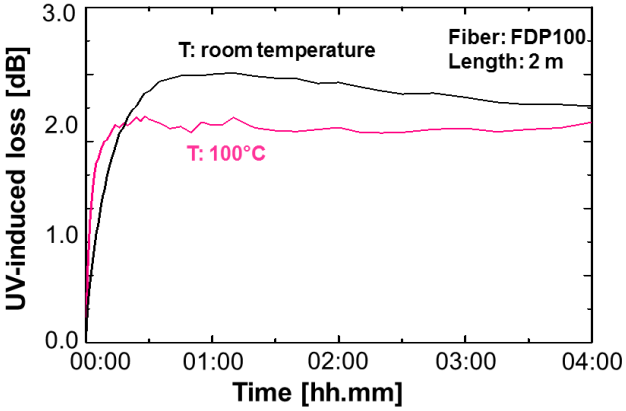

Fig. 10: *Temporal UV-damage at 214 nm wavelength of 2 m long FDP-fiber with 100 µm core, for different temperatures (room temperature, 100°C)*

4.5 Influence of temperature

Using fibers from the 1st generation, the UV-induced losses are strongly temperature-dependent. However in a 2 m long FDP-fibers with 100 µm core, as seen in Fig. 10, the 214 nm UV-induced losses after 4 h UV irradiation at 100°C is only 0.15 dB smaller in comparison to room temperature. The main difference is the slope at the beginning and the time duration for saturation, with and without an overshoot.

4.6 Influence of length

In order to study the length dependence of UV-induced loss (unit: dB) and attenuation (unit: dB/m) a 4 m long FVP-fibers with 100 µm core (1st generation) was gradually cut back in 0.5 m steps. After 4 h UV irradiation with the in-house light source system, the output power of each of the 8 equal fiber sections with 0.5 m lengths were measured and compared to a fresh and non-solarized sample of the same length. The spectral induced losses (sample # 1 ... 8) along the 4 m fiber were determined according to eq. 1 (Fig. 11). It is obvious, that the main UV absorption band at 214 nm is decreasing strongly with increasing number of the sections and the increasing position along the fiber (Fig. 12): the starting value of 21.0 dB or 42.0 dB/m decreases to < 2.0 dB or < 4.0 dB/m at fiber position > 3.5 m. Based on Fig. 12, the exponential decay approximation leads to the following equation: α_{UV} (z) = 58.3 dB/m · exp(z/0.66 m) + 0.81 dB/m with the correlation coefficient r^2 = 0.992. Because of the dynamic range of the system (< 25 dB), the UV-induced loss of a 2 m long fiber over the whole wavelength region cannot be determined; however, adding the spectra of the first 4 samples resulted in an UV-induced loss at 214 nm of 39,8 dB (Fig. 13).
Using this testing procedure for a 5 m long FDP-fiber with 100 µm core diameter, the exponential decay approximation leads to the following: α_{UV} (z) = 0.85 dB/m · exp(z/0.96 m) + 0.56 dB/m with the correlation coefficient r^2 = 0.874.

In addition, several damaging tests have been carried out with different fiber lengths (Fig.14). For increasing lengths, the temporal behavior shows a: reduction of an overshoot, while time of saturation is increased. In addition, a non-proportional increase of starting slope and non-proportional increase of final value after 4 or 8 h is observed (see Fig. 15, too: the fit is based on a 2nd order power-law approximation).

The reason for these length-dependences is clearly shown in Fig. 16. The damaging spectrum below 200 nm is significantly reduced along the fiber because of the high basic attenuation of approx. 1.0 dB/m at 200 nm. The shown spectra at the beginning will be reduced by the damaging process, additionally.

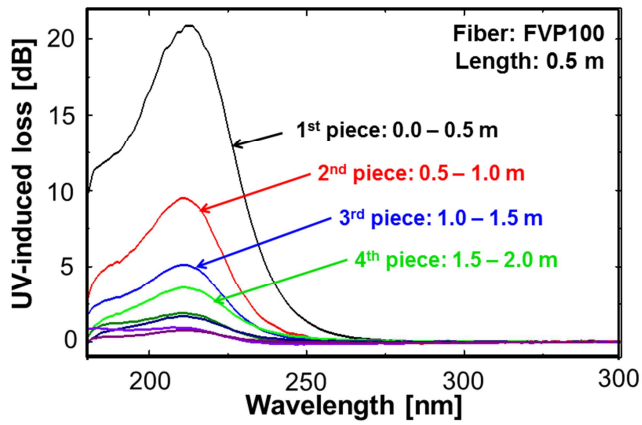

Fig. 11: *UV-induced losses after 4 h radiation in 0.5 m fiber sections of a 4 m long irradiated FVP fiber; the offsets of the loss spectra were adjusted at 330 nm and a slight wavelength shift (< 1 nm) was compensated using the D_β-peak*

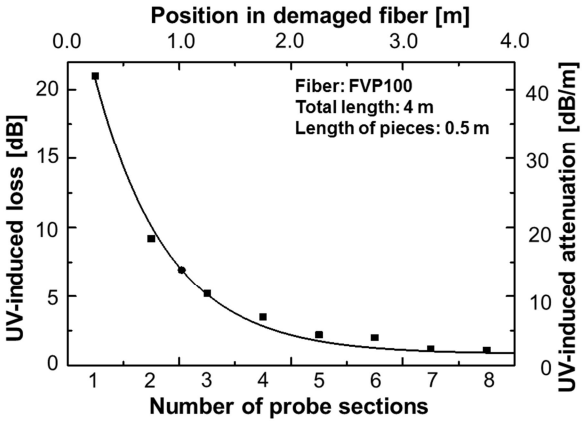

Fig. 12: *Measured UV-induced losses and attenuation at 214 nm along a 4 m long FVP-fiber, using 0.5 m long sections, derived from Fig. 11*

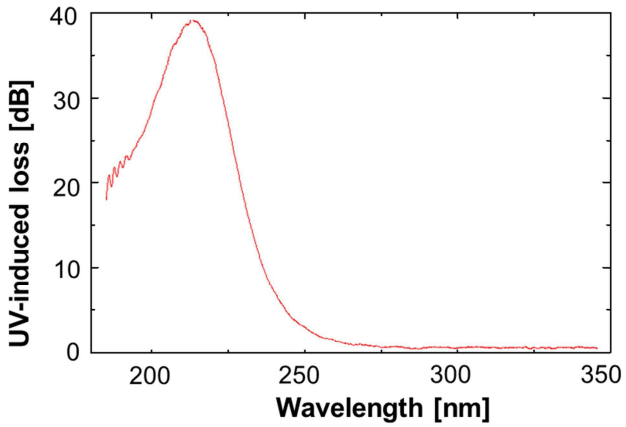

Fig. 13: *Calculated UV-induced losses in 2.0 m long irradiated FVP fiber, after 4 h radiation; the first four loss spectra (# 1-4) in Fig. 11&12 were added*

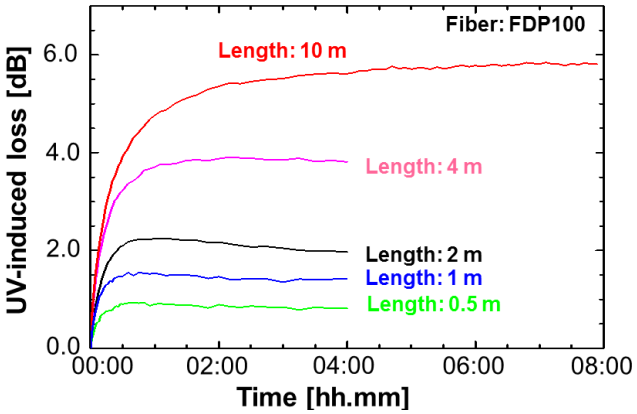

Fig. 14: *Temporal UV-damage at 214 nm wavelength of FDP-fiber with 100 µm core, for different fiber lengths; maximum and saturation are observed within 4 h UV irradiation for all fibers smaller than 4m*

4.7 Recovery

For intensity dependent applications, such as absorbance or fluorescence spectroscopy, the transient losses inducing system drifts have to be avoided or at least significantly reduced. Therefore, a recovery test is required (see Fig. 17).For this measurement, the shutter (Sh) in the setup (see Fig. 2) will be used in the recovery phase of 20 h (typical): the duration of UV light irradiation for testing irradiation is only 5 s to avoid additional damage, while the darkness phases are increasing with time, up to 30 minutes. After recovery, a continuous UV irradiation for 2 h is added to see the additional UV-induced loss. This second step of 0.25 dB leads to a slightly higher value of approx. 1.25 dB in comparison to the saturation value of 1.13 after 4 h irradiation. However, a (positive) signal drift in the recovery phase is observed after 12 h of testing which leads to a higher base level after 24 h, directly before the second damaging phase.

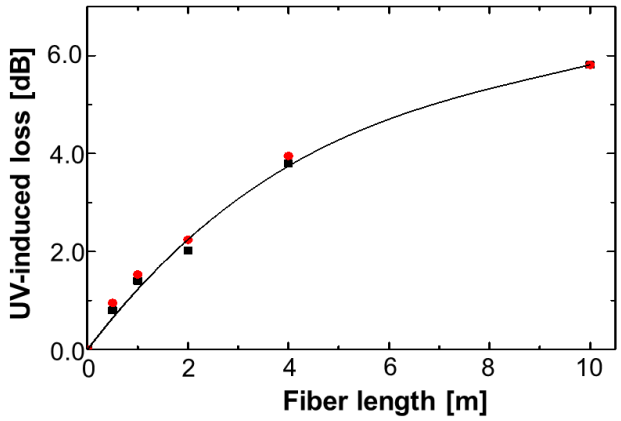

Fig. 15: *Maximum and final UV-damage at 214 nm wavelength of FDP-fiber with 100 µm core, for different fiber lengths, after 4 h or 8 h UV-irradiation.*

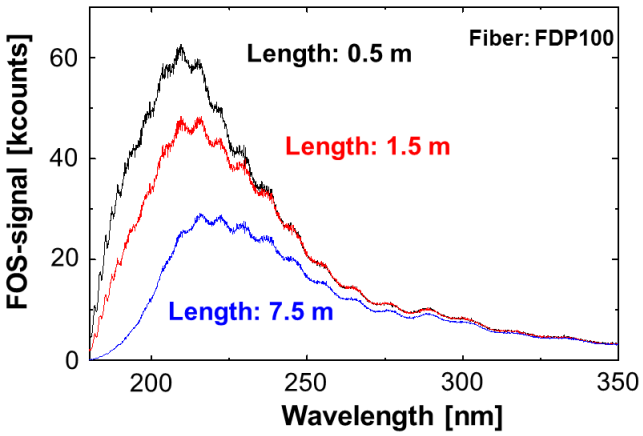

Fig. 16: *Measured FOS-signal related to output power of FDP-fiber with 100 µm core, for different fiber lengths; the output power describe the power distribution along the fiber due to basic attenuation and length-dependent UV-induced losses.*

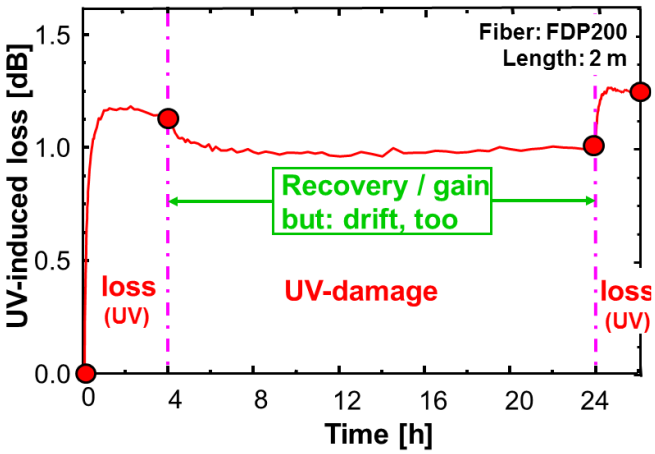

Fig. 17: *Temporal UV-damage and recovery at 214 nm loss due to 4 h deuterium lamp UV-irradiation, 20 h recovery (darkness; only 5 s UV-irradiation for measuring) and additional 2 h UV-irradiation*

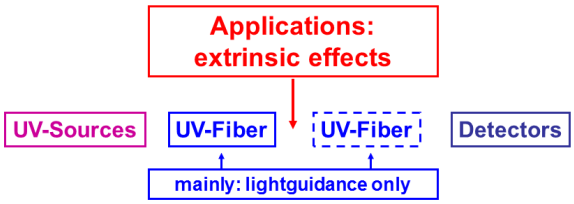

Fig. 18: *Overview of a fiber-optic system for UV-applications based on multi-mode silica fiber*

5. APPLICATIONS IN UV WAVELENGTH REGION

5.1 Overview about fiber-optic UV system

A typical setup for extrinsic sensor applications is shown in Fig. 18. Several UV light sources like broadband D_2 lamp, pulsed Xenon lamps, excimer-lasers or Nd:YAG laser with higher harmonics have be used. The detector system can be a spectrometer, a silicon detector or a photomultiplier tube. Adjusting the components to the applications, the following applications were demonstrated: Fiber optic spectrometer with cross-section converters [8,9], Diode-array (DA) TLC-method [10], DUV-dipping probe [11], Liquid-Core Waveguides [12], UV gas analyses with Hollow-Core-Waveguides [13,14], UV Resonant Raman Spectroscopy [15], Laser-induced fluorescence (LiF) [16], ocean color detection [17] and process control [18]

In the following, two additional UV-light sources as interesting candidates for new UV fiber-optic applications will be introduced. In contrast to the deuterium lamps, sufficient power output can be achieved with these light-sources even with UV-fibers having small core diameters (≤ 100 µm). The spectrum of a new broadband Xenon plasma source, the Laser Driven Light Source (LDLS EQ-99) manufactured by Energetiq [33] and the high pulse-power 355 nm Nd:YAG laser [34] are shown in Fig. 19.

5.2 UV damage with high-power broadband lamp, from 190 up to 2100 nm wavelength

As shown in Fig. 19, the spectral power of the new light source is significantly higher compared to deuterium lamp. In more detail, the gain is at least 22 dB at 200 nm and 45 dB at 600 nm [31]. Using LDLS, the temporal behavior and the steady-state spectral UV-induced losses are quite different (Fig. 20&21) to the above results, e.g. in Fig. 9. First of all, there is a significant increase of E'- and NBOH centers for the first 3 minutes; the slope at the beginning is in the order of 1 dB/min at 214 nm. After the maximum values of 1.75 dB at 214 nm, the saturation level of 0.65 dB at 214 nm will be reached after 4 h continuous irradiation. Looking above 240 nm in Fig. 20, the UV-induced losses have a maximum followed by an additional minimum after approx. 1.0 h and a slow increase, which is still going on after 4 h. The slope at 260 nm after 4 h is still in the order of 0.002 dB/min. Fig. 20 shows the whole loss spectra due to UV-damage after 1 min and 4 h of continuous irradiation. After 4 h, there is a spectral plateau from 235 nm up to 270 nm with the value of approx. 0.5 dB.

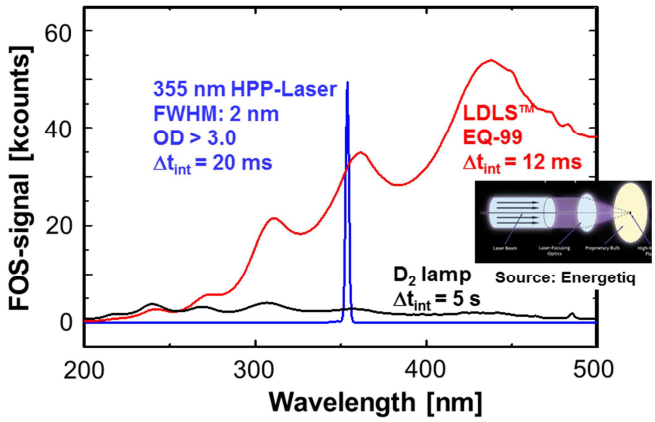

Fig. 19: *Overview about two interesting UV light sources for fiber-optic UV applications: the Laser Driven Light-Source [33] and the high pulse-power 355 nm laser [34]*

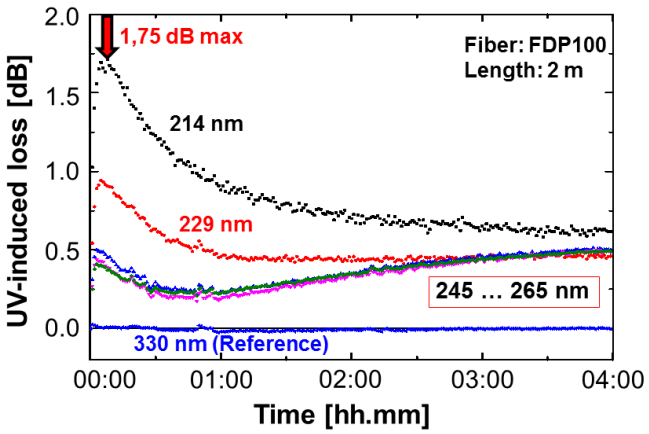

Fig. 20: *Temporal UV-damage at 214, 229, 245 … 265 & 330 nm wavelength of a 2 m long FDP-fiber with 100 µm core, for the new broadband LDLS*

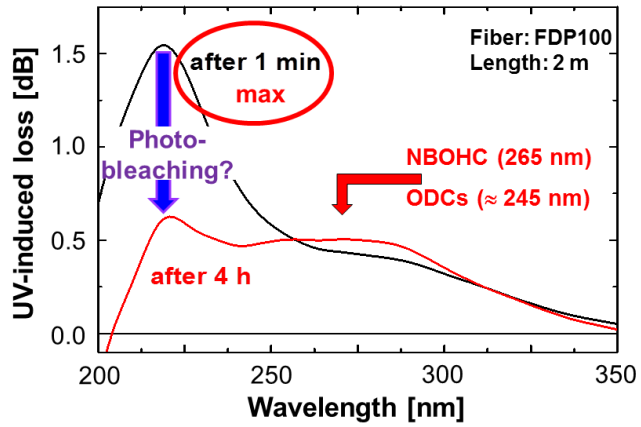

Fig. 21: *Spectral UV damage of a 2 m long FDP-fiber with 100 µm core, after 1 min and 4 h UV-irradiation with the new broadband LDLS, using the same raw data as in Fig. 21*

The damaging process with the high-power broadband light-source is quite different. After a very quick damage (less than 10 minutes), the spectral losses below 235 nm are decreasing to a significantly lower saturation value in respect to the values with deuterium lamp. This unexpected annealing effect can be explained with the spectral power of the light-source in the VIS- or IR-region. As seen in many photo-bleaching studies [27,35, 36] after Gamma-ray exposure, the induced losses can be reduced faster with a light source in parallel. Especially, undoped silica is very sensitive to photo-bleaching. To our knowledge, this effect has not been studied in detail, in the past. Therefore, further studies are in planning.

5.3 UV damage with 355 nm pulsed Nd:YAG lasers at cryogenic temperatures

There is an increasing interest in delivery systems at lower temperatures (liquid nitrogen, liquid helium), e.g. to study the stability of superconducting strands around 4 K [37,38].

In order to study the fiber behavior at cryogenic temperatures, the following setups for 77 K (liquid nitrogen) with modular components have been built up (Fig. 22). The Nd:YAG high pulse power laser system (Flare; Innolight [34]) as the light source LS has the following parameters: 355 nm wavelength, 90 µJ maximum pulse energy, 10 ns pulse width and a maximum repetition rate of 200 Hz. Using an imaging system IS, the laser beam was coupled into the fiber under test FuT. A Dewar flask with liquid nitrogen sustained the FuT with a well-defined bent and two straight sections of approximately 0.2 m at 77 K. Further, two feeding sections with lengths $L_{RT,I}$ of typically 0.3 m were kept necessarily at room temperature. The distal end of the FuT was mounted in front of a detector system DS; either a thermopile power meter (PS19Q, Coherent, Inc. [39]) or a pyroelectric detector (PEM100, LTB Berlin GmbH [40]) were used. The fiber end faces were fixed in SMA connectors (C). These connectors were mounted into SMA adapters, placed on translation stages. An attenuator (Att) and a shutter (Sh) were additionally in operation.

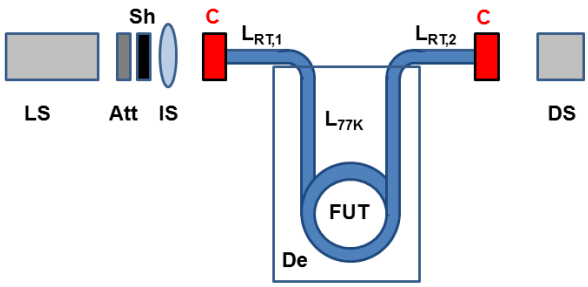

Fig. 22: *Setup for measurements at cryogenic temperatures (liquid nitrogen: 77 K); description see text*

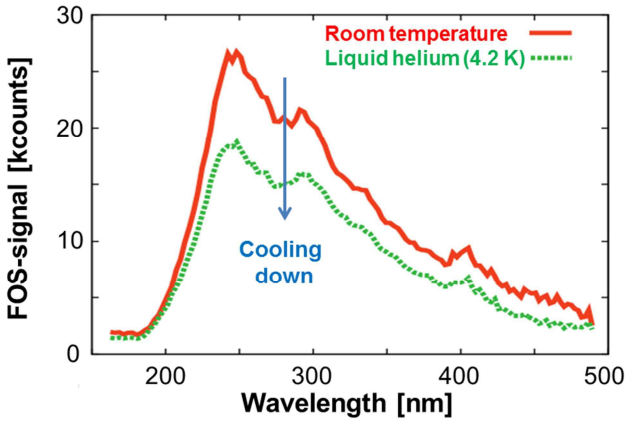

Fig. 23: *Signal reduction during cooling-down phase from room temperature down to 4.2 K in a 5 m long FDP fiber with 100 µm core diameter; a part of the fiber (< 1.0 m) will be kept at room-temperature*

For testing at 4.2 K, a similar system was used; more details are given in [37,38]. The length of the cooled section and the feeding fibers had to be adjusted. In these common studies, the bending losses of the 1.2 m long cooled fiber including 4 loops with 25 mm diameter during the cooling-down phase to 4.2 K or 3.5 m long fiber including multiple loops with were determined (Fig. 23). At 4 K, a nearly wavelength independent loss of approximately 1.6 dB at 4.2 K was measured caused by micro-bending due to the mismatch of thermal expansion of polyimide coating and silica fiber at 4.2 K [37]. This value is smaller than expected. In the studies at 77K, we have not seen any thermal losses in the cooling-down phase; however, a small increase below 200 nm was observed [41].

The UV-induced loss after 12 h UV irradiation of the Nd:YAG laser is shown in Fig. 24, for 4.2 K; the starting spectrum comparable to the spectrum after cooling-down in Fig. 24 and the final spectrum have been measured with a broadband D_2 lamp and a spectrometer, similar to set-up in Fig. 2. Only damage was observed below 300 nm, with absorption bands at 214 and 265 nm.

In addition, more detailed measurements at 77 K have been carried out [41]. As shown in Fig. 26, the UV-induced loss in a 5 m long fiber depends on the pulse energies of the 355 nm Nd:YAG laser. For lower pulse energies mainly the 214 nm optical absorption band appeared, similar in spectral shape with the D_2 lamp damaging. However, the 265 nm absorption band is generated with one order of magnitude higher pulse energies. Details of further studies are shown in [41].

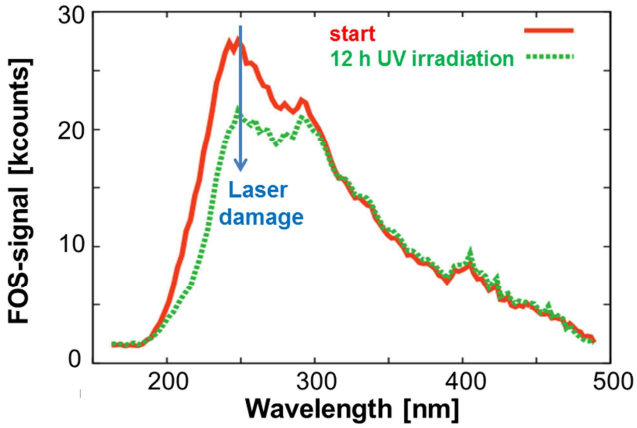

Fig. 24: *Signal reduction at 4.2 K in a 5 m long FDP fiber with 100 µm core diameter; a part of the fiber (< 1.0 m) will be kept at room-temperature due to 12 h UV irradiation using a high power pulsed 355 nm Nd:YAG laser*

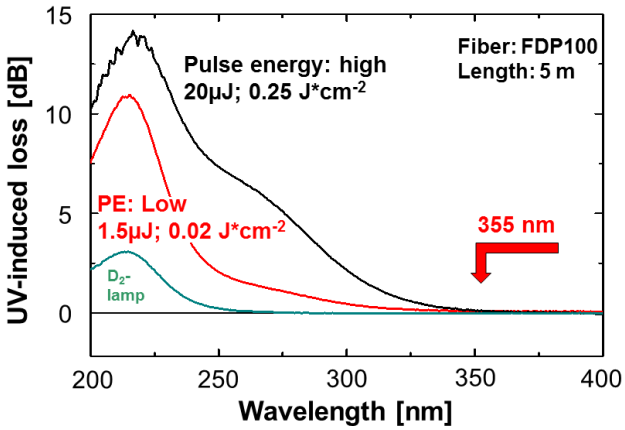

Fig. 25: *Spectral damage in 5 m long FDP fiber with 100 µm core diameter at cryogenic temperature of 77K, using the deuterium lamp and the pulsed Nd:YAG laser with different pulse energies; a part of the fiber (< 1.0 m) will be kept at room-temperature*

6. SUMMARY

In this paper, UV-damage in silica based UV-fibers due to defects in synthetic high-OH silica has been described in detail. Starting from the manufacturing process of UV fibers with synthetic silica core and fluorine doped cladding, the improvements of the UV fibers in regards to UV resistance over more than two decades have been demonstrated. To show the improved properties, an adequate measurement technique with D2 lamp was designed. For the first time, the main parameters and their influences on the UV induced losses were discussed. Because no standards for UV fiber testing exist to this date, this data can be used as a defining a standard test system.

In addition to existing UV applications, two new applications with new light sources have been introduced. For the first time, photo-bleaching in the UV-region in the presence of UV damage with broadband light-source, from UV up to NIR, has been demonstrated. For applications at cryogenic temperatures, on the other hand, first results were generated. The tested UV fibers, coated with Polyimide, can be used down to 4.2 K. In addition to bending losses during the cooling-down phase (< 1.6 dB for 1.2 m long cooled section), the level of UV-induced optical absorption after 4 or 12 h delivery of UV light is acceptable at lower temperatures.

7. ACKNOWLEDGEMENT

We would like to thank J. Clarkin (Polymicro Technologies, Phoenix), S. Unger and J. Kirchhof (IPHT, Jena) for fruitful discussions. In addition, we acknowledge the support for activities at cryogenic temperature by E. Takala (temporarily at CERN) and for testing some of the samples by T. Eifler (TransMIT, Friedberg).

8. REFERENCES

[1] M.Belz, H.-S.Eckhardt, C.P. Gonschior, G.Nelson, K.-F.Klein: “Quality control of UV resistant fibers for 200-300 nm spectroscopic applications”.SPIE-Proc.Vol. 6852 (BiOS 08), paper 6852-33 (San Jose, Jan. 2008)

[2] V.Kh.Khalilov, K.-F.Klein, J.Belmahdi, R.Timmerman, G. Nelson: “High-OH fibers with higher stability in the UV-region”. SPIE-Proc. BiOS‘06, Vol. 6083, paper 6083-08 (San Jose, USA, Jan.06)

[3] K.F.Klein,P.Schliessmann,E.Smolka,M.Belz,W.J.O.Boyle,K.T.V.Grattan: "UV-stabilized silica based fiber for application around 200 nm wavelength". Sensors and Actuators B, Vol. 38-39, pp. 305-309 (1997)

[4] M. Huebner, H. Meyer, K.-F. Klein, G. Hillrichs, M. Ruetting, M. Veidemanis, B. Spangenberg, J. Clarkin, G. Nelson: „Fiber-optic systems in the UV-region“. SPIE-Proc. BiOS‘00, Vol. 3911, pp. 303-312 (San Jose, Jan. 2000)

[5] V.Kh.Khalilov, K.-F.Klein, G.Nelson: “Low-OH all-silica fiber with broadband transparency and radiation resistance in the UV-region”. SPIE-Proc. BiOS‘04, Vol. 5317, paper 5317-9 (San Jose, Jan.04)

[6] Polymicro Technologies, Phoenix (USA): Data sheets about All-Silica Fibers (www.polymicro.com)
[7] Heraeus Quarzglas, Hanau (Germany): Brochures about Suprasil™ and Fluosil™ (www.heraeus.com)
[8] tec5 AG, Oberursel (Germany): Data sheets about Fiber-Optic Spectrometer (www.tec5.de)
[9] J&M Analytik AG, Essingen (Germany): Data sheets about Fiber-Optic Spectrometer (www.j-m.de)
[10] B.Spangenberg, K.-F.Klein,: „Fibre optical scanning with high resolution in thin-layer chromatography". J.Chromatogr. A, 898, 265-269, 2000
[11] World Precision Instruments, Inc., Sarasota (USA): Datasheets about Dipping Probes (www.wpiinc.com).
[12] M. Belz, "Simple and Sensitive Protein Detection System using UV LEDs and Liquid Core Waveguides", Advanced Environmental, Chemical, and Biological Sensing Technologies V, Optics East, Boston, 2007, Proc. of SPIE Vol. 6755, 675505
[13] H.-S. Eckhardt, K.Graubner, K.-F. Klein,T.Sun, K.T.V.Grattan, "Fiber-optic based gas sensing in the UV region", SPIE-Proc., Vol. 6083, paper 6083-35,2006
[14] H.-S. Eckhardt, L. Lagesson-Andrasko c, V. Lagesson, K.-F. Klein, K.T.V.Grattan: "Towards a fiber-optic detection device for GC-UV". Proc. of "29th international symposium on capillary chromatography" and "3rd GCxGC symposium", 2006
[15] L.S.Greek, H.G.Schulze, M.W.Blades, C.A.Haynes, K.-F.Klein,R.F.B.Turner, „Fiber-optic probes with improved excitation and collection efficiency for deep-UV Raman and resonance Raman spectroscopy". Appl.Optics, Vol.37, 170-180, 1998
[16] P. Karlitschek, "Fiber-optic studies related to UV-laser-based sensor for pollutants (in German)", ISBN-10: 3895888281, Cuvillier publisher, Goettingen, 1998
[17] R.L. Miller, M. Belz, C. Del Castillo, R. Trzaska, „Determining CDOM Absorption Spectra in Diverse Aquatic Environments Using a Multiple Pathlength, Liquid Core Waveguide System", Continental shelf research - Vol. 22, Issue 9, 1301-1310 (2002)
[18] Karl-Friedrich Klein, Joachim Mannhardt, Mathias Belz, Cornell Gonschior, Hanns S. Eckhardt, „Optical fibers in instrumental UV-analytics (Invited Paper)".,SPIE-Proc., Vol. 7173, paper 7173-36 (2009)
[19] K.-F.Klein,G.Hillrichs,P.Karlitschek,K.Mann: "Possibilities and limits of optical fibers for the transmission of excimer laser radiation". SPIE-Proc. Vol.2966 „Annual Boulder Damage Symposium", pp.564-573 (1996)
[20] G.H.Sigel jr.: "UV spectra in silicate glasses". J.-Non-Cryst.Solids, Vol. 13, pp. 372-398 (1973/74)
[21] D.L.Griscom: „Defect structures of glasses". J.Non-Cryst. Solids. Vol. 73, pp. 51-78 (1985)
[22] E.J.Friebele, D.L.Griscom: "Radiation effects in glass" in "Treatise on material science and technology". Acad.Press, New York, pp. 257-351 (1979)
[23] E.J.Friebele, et.al.: "Overview about Radiation Effects in Fiber Optics". SPIE-proc. 541, pp. 70 (1985)
[24] R.A.Weeks: "The many varieties of E'-centers: a review". J.-Non-Cryst.Solids, Vol. 179, pp. 1-9 (1994)
[25] L.Skuja: "Optically active oxygen-deficiency-related centers in amorphous silicon dioxide". J.-Non-Cryst.Solids, Vol. 239, pp. 16-48 (1998)
[26] V.Kh.Khalilov, G.A.Dorfman, E.B.Danilov, M.I.Guskov, V.E.Ermakov: "Character, mechanism of formation and transformation point defects in type IV silica glass". J.-Non-Cryst.Solids, Vol. 169, pp. 15-28 (1994)
[27] R.West: "Radiation effects on fibre optics". SPIE-Proc. Vol. 867, pp. 2-9 (Nov. 1987, Cannes, France)
[28] Heraeus Noblelight GmbH, Hanau (Germany): Brochure about deuterium-lamps (2002)
[29] Ocean Optics, Dunedin, FL (US), "Data sheet about fiber-optic spectrometer"
[30] K.-F.Klein, R.Kaminski,S.Hüttel, J.Kirchhof, S.Grimm, G.Nelson: "Lifetime improvements and of UV-improved fibers for new applicatons". SPIE-Proc.Vol. 3262C (BiOS'98), pp. 150-160 (San Jose, Jan. 1998)
[31] J. Heimann, K,-F. Klein, C.P. Gonschior, M. Klein, G. Hillrichs, "Optical fibers for 355 nm pulsed lasers and high-power broadband light sources", SPIE Proc., Vol. 8576, paper 8576-19, 2013
[32] Hamamatsu, Hamamatsu (Japan), "Data sheets about deuterium lamps"
[33] Energetiq, Woburn (USA): "Data sheets about Laser-Driven Light-Source (www.energetiq.com)
[34] Innolight (former Lumanova), Hannover (Germany), "Data sheet about diode-pumped semiconductor lasers"
[35] E.J.Friebele, M.E.Gingerich: "Photobleaching Effects in Optical Fiber Waveguides". Appl.Optics, Vol.20, pp.3448 (1981)
[36] G.Breuze, J.Serre, A.Friant: "Selective photobleaching of steady-state Gamma irradiated silica fibers applications to the hardening of a digital link". SPIE-Proc. Vol. 867, pp. 32-39 (Nov. 1987, Cannes, France)
[37] E. Takala et al.,"Silica-Silica Polimide Buffered Optical Fiber Irradiation and Strength Experiment at Cryogenic Temperatures for 355 nm Pulsed Lasers," Cryogenics, 52, 77-81, 2011.
[38] E.Takala: "The Laser quenching technique for studying the magneto-thermal instability in high critical current density superconduction strands for accelerator magnets". ISBN 978-951-29-5128-4, PhD-thesis, University of Turku (Finland, 2012
[39] Coherent, Santa Clara, CA (US), "Data sheet about detector systems for lasers"
[40] LTB, Berlin (Germany), "Data sheet about detector systems for lasers"
[41] J.C. Heimann, C P. Gonschior, K.-F. Klein, G. Hillrichs, E, Takala, „Spectral UV losses in 355 nm pulsed laser delivery system at low temperatures", J.Non-Cryst. Solids, for review